CLASSIFICATION OF VEGETATION ABOVE THE TREE LINE IN THE KRKONOŠE MTS. NATIONAL PARK USING REMOTE SENSING MULTISPECTRAL DATA

RENÁTA SUCHÁ, LUCIE JAKEŠOVÁ, LUCIE KUPKOVÁ, LUCIE ČERVENÁ

Charles University, Faculty of Science, Department of Applied Geoinformatics and Cartography, Prague, Czech Republic

ABSTRACT

This paper compares suitability of multispectral data with different spatial and spectral resolutions for classifications of vegetation above the tree line in the Krkonoše Mts. National Park. Two legends were proposed: the detailed one with twelve classes, and simplified legend with eight classes. Aerial orthorectified images (orthoimages) with very high spatial resolution (12.5 cm) and four spectral bands have been examined using the object based classification. Satellite data WorldView-2 (WV-2) with high spatial resolution (2 metres) and eight spectral bands have been examined using object based classification and per-pixel classification. Per-pixel classification has been applied also to the freely available Landsat 8 data (spatial resolution 30 metres, seven spectral bands). Of the algorithms for per-pixel classification, the following classifiers were compared: maximum likelihood classification (MLC), support vector machine (SVM), and neural net (NN). The object based classification utilized the example-based approach and SVM algorithm (all available in ENVI 5.2). Both legends (simplified and detailed ones) show best results in the case of orthoimages (overall accuracy 83.56% and 71.96% respectively, Kappa coefficient 0.8 and 0.65 respectively). The WV-2 classification brought best results using the object based approach and simplified legend (68.4%); in the case of per-pixel classification it was the SVM method (RBF) and detailed legend (60.82%). Landsat data were best classified using the MLC (78.31%). Our research confirmed that Landsat data are sufficient to get a general overview of basic land cover classes above the tree line in the Krkonoše Mts. National Park. Based on the comparison of the data with different spectral and spatial resolution we can however conclude that very high spatial resolution is the decisive feature that is essential to reach high overall classification accuracy in the detailed level.

Keywords: vegetation above the tree line, Krkonoše Mountains, object based classification, per-pixel classification, multispectral data

Received 12 October 2015; Accepted 25 November 2015

1. Introduction

The Krkonoše Mountains is a mountain range with a fragmented alpine zone that occupies a narrow span of elevations and has developed into two separated areas. The highest parts of the Krkonoše Mts. National Park (KRNAP) rise above the tree line and are covered by relict tundra. These areas are included in the international tundra monitoring program (INTERACT: International Network for Terrestrial Research and Monitoring in the Arctic) (Soukupová et al. 1995; Jeník and Štursa 2003).

For vegetation mapping and related analyses in large, isolated areas that often receive legal protection, such as tundra, remote sensing methods are commonly used. Data with various spatial and spectral resolutions are analysed using different methods of per-pixel and object based classification.

Regarding the vegetation classification above the tree line, Král (2009) classified the orthoimages with infrared band with spatial resolution 0.9 metres using the maximum likelihood algorithm in Jeseníky Mountains. Král (2009) especially focused on transitional zones between subalpine forests and alpine tundra. In this way, he defined seven land cover classes: anthropogenic areas, pastures and barren land, *Pinus mugo* scrub, deciduous trees, spruce cultures, dry spruce stands, and rocks. The overall accuracy equalled 78%.

Orthoimages were also examined by Müllerová (2005) who studied the tundra vegetation in the Krkonoše Mts. National Park. Having used multispectral aerial data and the maximum likelihood method, she defined seven classes: *Pinus mugo* scrub, *Nardus stricta* stands, subalpine tall grasslands and tall-herb vegetation, vegetation along roads, roads, water areas, and wetlands. The overall accuracy equalled 79%. The use of unsupervised classification (ISODATA method) brought overall accuracy of 63% and six classes were identified.

Zagajewski et al. (2005) conducted mapping in the eastern part of the Tatra National Park, Poland. They focused on the mountain vegetation of subalpine, alpine, and sub-nival zones utilizing hyperspectral data and maximum likelihood and neural net methods. Hyperspectral aerial images were acquired by DAIS 7915 and by ROSIS sensors. Based on unsupervised classification and visual interpretation of the images, seven classes for supervised classification were defined: *Pinus mugo* scrub, forests, meadows, rocks, lakes, shadows, and roads. Overall accuracy reached 71–85%. Hyperspectral data were used also by Marcinkowska et al. (2014). They classified vegetation communities in the Krkonoše Mts. National Park using APEX data and Support Vector Machines classifier.

http://dx.doi.org/10.14712/23361980.2016.10
Suchá, R. – Jakešová, L. – Kupková, L. – Červená, L. (2016):
Classification of vegetation above the tree line in the Krkonoše Mts. National Park using remote sensing multispectral data
AUC Geographica, 51, No. 1, pp. 113–129

Object based classification was used by Laliberte et al. (2007) in order to distinguish between green and aging vegetation in New Mexico. The study area was located about 1,200 metres a. s. l. They combined the methods of decision tree and nearest neighbour. The classification accuracy equalled 92%. Object based classifications of orthoimages was also used by Lantz et al. (2010) in order to examine changes in vegetation characteristics (cover and patch size) across a latitudinal gradient in the Mackenzie Delta Uplands. Four classes were identified: shrub tundra, dwarf shrub tundra, water, and bare ground, with overall accuracy 78.1% (Kappa coefficient 0.66).

All of the above-mentioned studies used data with very high spatial resolution. Data collected by Landsat sensors (one pixel equals to 30 × 30 metres) are commonly used to produce land cover classifications in large areas (see Dixon, Candade 2008) or to examine forest cover (Wolter et al. 1995, etc.). Landsat data, however, are only rarely used for examination of grassland vegetation, except in the case of vast regions in the northern tundra (Johansen et al. 2012; Pattison et al. 2015).

Several authors compared a number of pixel classification algorithms (Zagajewski 2005) or per-pixel and object based classification – see Yu et al. (2006), Cleve et al. (2008), or Myint et al. (2011). So far, no study has been carried out that would compare the potential of different multispectral data and different types of classification algorithms, including comparison of object based and per-pixel approach for classification of alpine vegetation. Thus, our study aims at evaluation and comparison of selected multispectral data with various spatial and spectral resolutions for land cover classification above the tree line (focus is put on different vegetation classes), using different classifiers including object based image analysis (OBIA) and per-pixel approach. Orthoimages can serve as an example of very high resolution data in this study. Data collected by WorldView-2 satellite show high spatial and spectral resolutions; the freely available data collected by Landsat 8 (moderate resolution) are also examined.

As different vegetation types cover only small patches of land, it is expected that spatial resolution of the data may be crucial for the classification. On the other hand, different vegetation types are clearly confined and usually do not overlap. Thus, we presume that the object based approach applied to high resolution data should bring more accurate results than the per-pixel approach.

2. Study Area

Arctic-alpine tundra occurs in the highest parts of the Krkonoše Mountains above the tree line (from 1,300 m a. s. l. up). It covers a limited area of 47 km^2 (32 km^2 on the Czech territory, 15 km^2 on the Polish territory), i. e. just 7.4% of the total Krkonoše area. The Scandinavian Ice Sheet repeatedly expanded as far as to the northern foothills of the Krkonoše Mountains and during the Holocene, tundra was a permanent phenomenon here (Treml et al. 2008; Margold et al. 2011). As a result of this palaeogeographical history, the Krkonoše Mountains represent a "biodiversity crossroads" where Nordic and alpine flora and fauna coexist (Jeník and Štursa 2003).

The area covered by natural arctic-alpine tundra was expanding due to deforestation and grazing from Early Middle Ages (9th–11th century, Speranza et al. 2000; Novák et al. 2010) until the beginning of the 19th century when mountain agriculture (grazing and grass mowing) peaked (Lokvenc 1995). Direct human impacts then gradually diminished until the 1940s. Almost no direct human intervention in the tundra zone has occurred since then as these areas became strictly protected as nature reserves. The alpine vegetation is being occasionally disturbed mainly by periodical avalanches and debris flows. Closed alpine grasslands, subalpine tall grasslands, *Pinus mugo* scrub, alpine and subalpine scrub currently form the prevailing vegetation types; in the highest altitudes also mosses, lichens, and alpine heathlands are common (Chytrý et al. 2001).

Two spatially separated parts make up the study area: Western Tundra and Eastern Tundra (Figure 1). The western part is situated near Labská bouda and covers about 1,284 hectares. The Eastern part is located around Luční bouda covering 2,284 hectares.

Both parts of tundra on the Czech territory were examined in full using the Landsat data. Classifications of the other data sources have been executed only in selected parts of the study area (565 hectares in the western part, 839 hectares in the eastern part) – Figure 1. Classifications using the detailed legend were applied only in the western area.

3. Data and Methods

3.1 Data

Three sensors of different spectral and spatial resolution represent multispectral data in this study. First, there are orthoimages acquired by aerial sensor on June 18, 2012. Second and third are two satellite sensors: WordView-2 and freely available Landsat 8. The WordView-2 images were acquired on July 22, 2014 (western part) and on August 10, 2014 (eastern part). The Landsat 8 cloud-free image acquired on July 27, 2013 (ID: LC81910252013208LGN00) was chosen from the Landsat archive.

Table 1 shows basic information on the data. No atmospheric corrections were made as classifications were carried out separately for all images; consequently, such adjustments were not necessary (Song et al 2001). Spatial accuracy was secured by geometric corrections and orthorectification (orthoimages, WV-2) using digital surface model created from aerial laser data (cloud of points, 5 points/m^2) and L1T product in the case of Landsat

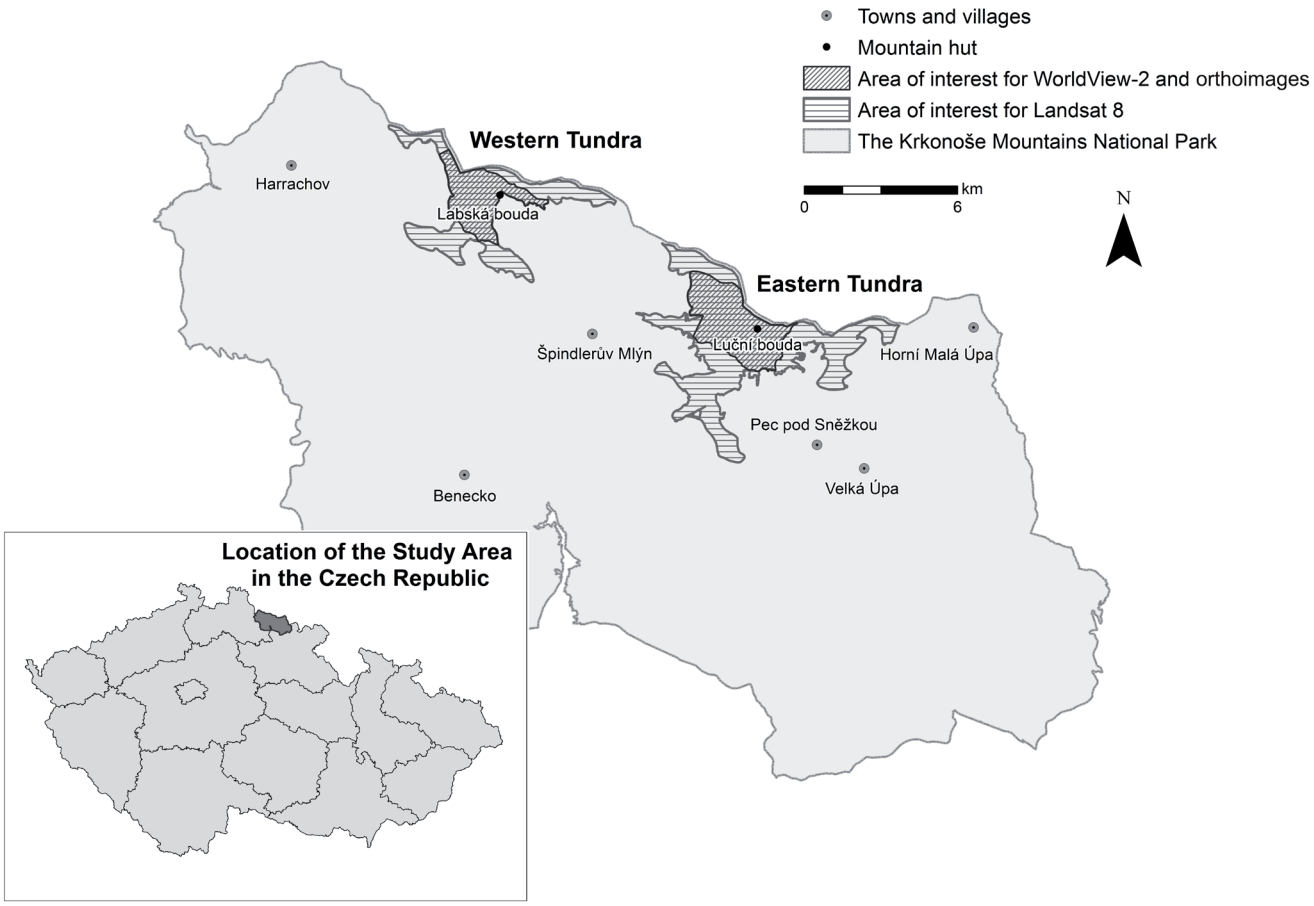

Fig. 1 Study area. Source: Authors

Tab. 1 Data parameters.

Data	Spatial resolution (metres)	Number of bands used for classifications	Radiometric resolution	Date
Orthoimages	0.125	4 (blue, green, red, NIR)	8 bit	June 18th, 2012
WV-2	2	8 (coastal, blue, green, yellow, red, red edge, NIR, NIR2)	11 bit	July 22th, 2014; August 10th, 2014
Landsat 8	30	7 (coastal, blue, green, red, NIR, SWIR1, SWIR2)	12 bit	July 27th, 2013

data (the latter utilizes corrections of digital surface model and surface points GLS2000).

Fifty nine polygons corresponding to vegetation classes as defined in the legend were identified in the field. Data were collected in the period June 23 – June 25, 2014. Polygons were located by GPS (Trimble Geoexplorer 3000 Geo XT, accuracy 10 centimetres) and classified on the botanical basis according to the legend (see Chapter 3.2). Polygons corresponding to classes *Pinus mugo* scrub, *Picea abies* stands, water and block fields, and anthropogenic areas were added later using manual vectorization based on visual interpretation of orthoimages.

3.2 Classification Legend

Definition of the legend constitutes the crucial part of the research. Classifications were made using two types of legends: the detailed legend (12 classes, respectively 13 for OBIA – Figure 3) for orthoimages and WV-2 data, and simplified one (8 classes, respectively 9 classed for OBIA – Figure 3) for all three types of data.

The detailed legend was created in cooperation with national park botanists and includes the most important classes of grassland vegetation as well as other vegetation classes, and also classes without any vegetation cover (Figure 2).

The detailed legend was used for orthoimages and WV-2 in the Western Tundra only. As many vegetation classes cover small patches of land less than 900 m^2 (equal to 1 pixel of Landsat 8), it became necessary to create a simplified legend suitable also for Landsat data classification. This simplified legend includes eight classes and was used for classification of all data types for the sake of comparison.

Block fields and anthropogenic areas

Picea abies stands

Pinus mugo scrub

Subalpine *Vaccinium* vegetation

Nardus stricta stands

Species-rich vegetation with high cover of forbs

Calamagrostis villosa stands

Molinia caeruela stands

Deschampsia cespitosa stands

Subalpine tall-herb vegetation

Alpine heathlands

Wetlands and peat bogs

Water areas

Fig. 2 Pictures of vegetation classes as defined in the legend.
Source: Authors

Detailed legend
1. Block fields and anthropogenic areas
2. *Picea abies* stands
3. *Pinus mugo* scrub
4. Subalpine *Vaccinium* vegetation
5. Closed alpine grasslands
5a. *Nardus stricta* stands
5b. Species-rich vegetation with high cover of forbs
6. Subalpine tall grasslands
6a. *Calamagrostis villosa* stands
6b. *Molinia caeruela* stands
6c. *Deschampsia cespitosa* stands
7. Subalpine tall-herb vegetation
8. Alpine heathlands
9. Wetlands and peat bogs
10. Water areas (only for OBIA)

Simplified legend
1. Block fields and anthropogenic areas
2. *Picea abies* stands
3a. *Pinus mugo* scrub dense (more than 80% of total cover)
3b. *Pinus mugo* scrub sparse (30–80% of total cover)
4. Closed alpine grasslands dominated by *Nardus stricta*
5. Grasses (except *Nardus stricta*) and subalpine *Vaccinium* vegetation
6. Alpine heathlands
7. Wetlands and peat bogs
8. Water areas (only for OBIA)

3.3 Training and Validation Data

The dataset collected in the field and completed with polygons added on the basis of orthoimages visual interpretation (see Chapter 3.1) was divided into training and validation parts.

Training dataset for per-pixel and object based classification of WV-2 and orthoimages using detailed classification legend contains 33 training polygons divided into 13 classes. The total area of training dataset is about 6,700 m^2.

Thirty seven polygons (area of 11,800 m^2) were used for validation. The training dataset for simplified legend was created by visual interpretation of orthoimages (WV-2 data, orthoimages). The total area of training data covered 17,396 m^2 (western part) and 31,800 m^2 (eastern part), respectively. For validation, combined validation and training datasets for the detailed legend (see above) re-classified into the simplified legend were utilized.

Training dataset for the simplified legend, based on visual interpretation of orthoimages, was also created in the case of Landsat 8 data. The rather big size of Landsat pixels, however, necessitated the use of larger areas. Altogether 1,133 pixels were trained (total area 1,019,700 m^2). The validation was again based on the dataset collected in the field (see Chapter 3.1). This dataset, however, had to be radically altered using visual interpretation of orthoimages and Landsat 8 images. The polygons identified in the field were always smaller than one Landsat 8 pixel. Thus, in cases when also the surrounding area was identified as the same class of the simplified legend, the respective pixels were taken into consideration in the accuracy assessment. On the contrary, pixels that clearly included a different land cover were deleted. Following the above mentioned adjustments, the Landsat validation dataset included 332 pixels covering the area of 298,000 m^2.

3.4 Mask

Clouds, shadows, and snow had to be masked from the imagery. The mask for WV-2 images was created by unsupervised classification ISODATA. Altogether 40 classes were identified and further aggregated into four groups: shadows and water areas in Western Tundra, plus clouds and snow in Eastern Tundra. The mask consisting of mentioned four classes had been applied to the imagery before the classification process started.

The mask applied to orthoimages (snow, shadows of vegetation and terrain) was created by object based classification using ENVI software and the rule-based approach. For the rules and attributes see Table 2. All four spectral bands and two parameters (Scale Level 40, Merge Level 80) were employed to carry out the segmentation.

For Landsat data, the mask of clouds and their shadows (located at NW part of the study area) was created using ISODATA classification.

Tab. 2 Rules and attributes used for orthoimages mask creation

Class	Attribute	Rule
shadows	Spectral Mean	1 < NIR < 65
snow	Spectral Mean	NIR > 255

3.5 Classification

The classification methods correspond to data types. Big differences among spatial resolutions of different data types justify the use of per-pixel and object based classification. Blaschke (2010) argues that the per-pixel approach brings better results when data with low spatial resolution are used; on the contrary, if data with high spatial resolution were available, object based classification is more appropriate. In our research, only object based classification is used for orthoimages, and only per-pixel classification for Landsat data. The WorldView-2 data were analysed using both object based and per-pixel approach enabling the comparison of results brought by these two methods. For schematic workflow see Figure 3.

3.6 Classification per-pixel

Three different per-pixel supervised classification algorithms were employed in this study: maximum likelihood

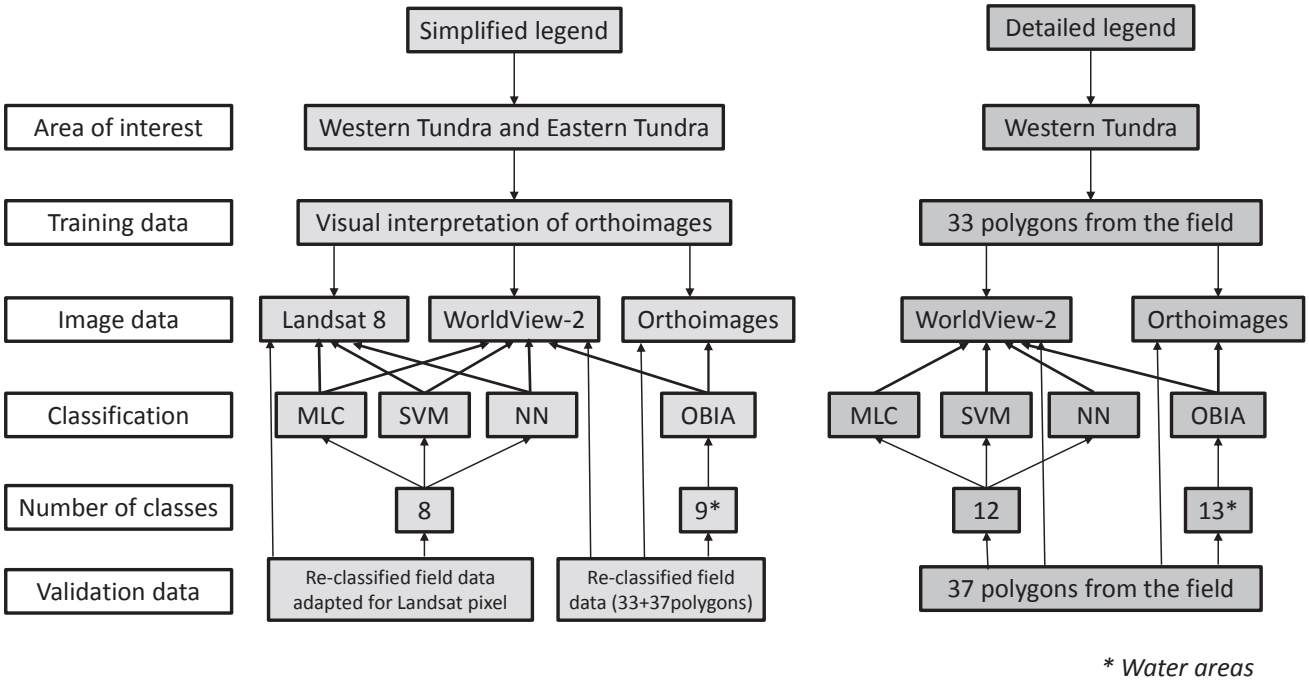

Fig. 3 Workflow.

classification (MLC), support vector machine (SVM), and neural net algorithms (NN).

Maximum likelihood classification

There are two conditions for successful application of this widely used algorithm. First, the image data should show normal distribution (Fernandez-Prieto 2006). Second, the training samples' statistical parameters (e.g., mean vector and covariance matrix) should truly represent the corresponding land cover class (Duarte et al. 2005). When ENVI software is used for maximum likelihood algorithm, parameters cannot be changed in any way with the exception of probability threshold parameter. The latter, however, was not used.

Machine learning algorithms

The machine learning classification algorithms, such as support vector machines (SVM) or artificial neural networks (or neural networks; NN), are also pixel-based classifiers (Petropoulos et al. 2012; Camps-Valls et al. 2004). Both methods belong among supervised non-parametric methods, which means that no particular data distribution is required (e.g. normal distribution). This makes a difference compared to other conventional classifiers, such as maximum likelihood classifier (Jones and Vaughan 2010). This fact is a big advantage of NN and SVM as the majority of remotely sensed data show an unknown statistical distribution.

Support vector machines algorithm

The support vector machines algorithm is based on the statistical learning theory and aims to find the best hyperplane in a multidimensional feature space that optimally separates classes. The term "best hyperplane" is used to refer to a decision boundary obtained in a training step and minimizing misclassifications. Training samples used for construction of hyperplane are called support vectors. These lie on the margin of classes to be classified and are extracted automatically by the algorithm (Jones and Vaughan 2010; Petropoulos et al. 2012; Mountrakis et al. 2011; Camps-Valls et al. 2004). Three Kernel types were tested using ENVI software in the case of SVM classification: radial basic functions (RBF), linear, and polynomial. In the case of RBF, Gamma was set to 0.125 for WV-2 and 0.143 for Landsat 8. Kernel Polynomial 2 was chosen in the case of polynomial function.

Neural networks algorithm

The artificial neural networks algorithm is designed to simulate human learning process by establishing linkages between input and output data via one or more hidden layers. The basic unit of each layer is called neuron (node) (Benediktsson et al. 1990). The classic model of a feed-forward multilayer neural network, known as multilayer perception (MLP) has fully-connected neurons between all layers (input, output, and hidden), which means that each neuron of a given layer feeds all the neurons in the next layer (Camps-Valls et al. 2004). This model is used in our processing tool, ENVI 5.2 software.

The neural network algorithm, applied to WV-2 data, was used in two modes. First, the default setting of ENVI software was applied. Second, the setting shown in Table 3 was used. Default setting was also applied to Landsat 8 data as the hidden layers and changes of some other parameters did not bring better results.

Table 3 Parameters of neural network algorithm

Training Threshold Contribution	0.9
Training Rate	0.9
Training Momentum	0.1
Training RMS Exit Criteria	0.05
Iteration	5000

3.7 Object based image classification

The object based image analysis (OBIA) does not examine pixels, but works with homogeneous clusters of pixels called segments. Segments are areas generated by one or more criteria of homogeneity. Thus, compared to single pixels, segments include additional spectral information (e.g. mean values per band, minimum and maximum values, mean ratios, variance etc.) (Blashke 2010). The example-based approach in ENVI software was employed for object based classification using the support vector machine algorithm.

Segmentation

The ENVI software includes only two segmentation algorithms: edge and intensity. The edge algorithm, where images are divided on the bases of Sobel's method of edge detection, was chosen in this study. Segmentation (orthoimages and WV-2) was carried out using all four/eight spectral bands. The parameters applied are shown in Table 4.

The ENVI software processes the segmentation each time it is started; consequently, the software does not allow to use any previously segmented image for further classifications.

Tab. 4 Segmentation parameters

Parameter	Orthoimages	WV-2
scale level	45	50
merge level	80	85
texture kernel size (pixels)	5 × 5	3 × 3

Example based classification

The example based classification sorts segments into pre-defined classes using training areas (segments), selected attributes, and classification algorithm. The following spectral and texture attributes were chosen: spectral mean, spectral max, spectral min, spectral standard deviation, texture mean, and texture variance. The above mentioned attributes were calculated for all spectral bands. The SVM classification algorithm with Kernel type radial basic function was used.

3.8 Accuracy Assessment

The ENVI software was used for accuracy assessment in all cases using validation polygons as defined for different data types (Chapter 3.3 and Figure 3). First, Confusion Matrix was created on the basis of ground true ROIs. The total accuracy was assessed as was the producer's and user's accuracy for different classes. Kappa coefficient for each classification was calculated, too.

4. Results

Table 5 shows the results of classifications (object based and per-pixel) for the detailed legend (applied in the western part of the tundra for orthoimages and WV-2 data). Table 6 shows the results for the simplified legend (applied in both parts of the tundra for all types of data). Figures 4–7 show the best classification map outputs for different types of data.

Tab. 5 Results of different classification methods (detailed legend) in Western Tundra.

Method	Data	Accuracy (%)	Kappa coeficient
OBIA-SVM (RBF)	orthoimages	**71.96**	0.65
	WV-2	**66.50**	0.60
SVM (RBF)	WV-2	60.82	0.54
SVM (polynomial)	WV-2	60.45	0.54
SVM (linear)	WV-2	60.30	0.54
NN	WV-2	60.13	0.54
MLC	WV-2	58.07	0.53
NN (default)	WV-2	54.59	0.49

4.1 Classification results: orthoimages

Orthoimages were classified by the object based approach only. This was applied to the detailed legend (western part) as well as to the simplified legend (western and eastern parts). The best classification results were obtained in the Eastern Tundra for simplified legend; the overall accuracy reached 83.56% (Kappa coefficient = 0.8). When different classes of the legend are compared, the classes "block field and anthropogenic areas", "water areas", and "wetlands and peatbogs" show the best results. The user's and producer's accuracy exceeded 90% in all cases.

On the contrary, the class "closed alpine grasslands dominated by *Nardus stricta*" shows the worst results of all. Though the producer's accuracy equalled 99.7%, the user's accuracy reached only 27%. The most common overlaps were with "*Pinus mugo* scrub sparse" and also with "wetlands and peatbogs".

In the case of detailed legend (Western Tundra), the overall accuracy equals 71.96% and Kappa coefficient 0.65. The best results were again achieved for the classes "water areas", "block fields and anthropogenic areas", and also for "*Pinus mugo* scrub". Producer's and user's accuracy varied in the range 87–100%. The classes "wetlands and peat bogs" and "subalpine *Vaccinium* vegetation" also show very good results with producer's and user's accuracy

Tab. 6 Results of different classification methods (simplified legend) in both parts of Tundra.

Method	Data	Area	Accuracy (%)	Kappa coefficient
OBIA-SVM (RBF)	orthoimages	East	**83.56**	0.8
	orthoimages	West	73.1	0.67
	WV-2	East	**66.37**	0.6
	WV-2	West	**68.4**	0.62
MLC	WV-2	East	57.04	0.48
	WV-2	West	59.96	0.51
	Landsat	West/ East	**78.31**	0.75
SVM (polynomial)	WV-2	East	42.49	0.39
	WV-2	West	56.11	0.46
	Landsat	West/ East	68.37	0.63
SVM (RBF)	WV-2	East	42.82	0.35
	WV-2	West	56	0.46
	Landsat	West/ East	68.67	0.64
SVM (linear)	WV-2	East	41.19	0.32
	WV-2	West	55.28	0.45
	Landsat	West/ East	68.37	0.64
NN (default)	WV-2	East	41.71	0.33
NN (default)	WV-2	West	57.42	0.47
NN	WV-2	East	36.64	0.27
NN	WV-2	West	58.36	0.48
NN (log)	Landsat	West/ East	63.55	0.58

ranging between 70% and 80%. On the contrary, the classes "alpine heathlands", "*Calamagrostis villosa* stands", and "*Deschampsia cespitosa* stands" show poor accuracy (less than 10%). In the case of alpine heathlands, the selected sample did not include enough training areas.

4.2 Classification results: WV-2 data

Per-pixel and object based approaches were used in the case of WV-2 data. Both classifications were applied to detailed legend (Western Tundra) as well as to simplified legend (Western and Eastern Tundra).

Best results were obtained in the case of object based classification applied to simplified legend in the western part (overall accuracy = 68.4%, Kappa coefficient = 0.62). Classes "*Picea abies* stands" and "block fields and anthropogenic areas" were classified with the highest accuracy. Producer's and user's accuracy varied in the range 90–100%. Very good results were also obtained in the case of "grasses (except *Nardus stricta*) and subalpine *Vaccinium* vegetation" with producer's and user's accuracy equalling ca. 80%. "*Pinus mugo* scrub dense" was often confused with "*Pinus mugo* scrub sparse". The class "closed alpine grasslands dominated by *Nardus stricta*" shows the worst results (producer's accuracy = 73.73%, user's accuracy = 35.51%).

The overall accuracy of object based classification in the western part (detailed legend) was almost identical to that in the eastern part (simplified legend) – around 66%, Kappa coefficient = 0.6). Producer's and user's accuracy reached almost 100% in the case of "block fields and anthropogenic areas" class. Also the classes "*Pinus mugo* scrub" and "*Picea abies* stands" showed very good results (producer's and user's accuracy 80–99%). As in the case of orthoimages, the classes "alpine heathlands", "*Calamagrostis villosa* stands", and "*Deschampsia cespitosa* stands" were classified with poor accuracy (producer's and user's accuracy below 5%).

Per-pixel classifications of WV-2 brought worse results than the object based one. Overall accuracy ranged between 50 and 60%. As regards the detailed legend (Western Tundra), the SVM (RBF) classification brought the best results (60.82%, Cappa coefficient = 0.54). The MLC method worked best for the simplified legend (59.96%, Cappa coefficient = 0.51).

Classes "*Pinus mugo* scrub" (producer's accuracy = 85.35%, user's accuracy = 76.49%) and "block fields and anthropogenic areas" show best results within the detailed legend classified by per-pixel approach (SVM RBF method). Also "subalpine *Vaccinium* vegetation" was classified well (producer's accuracy = 70.26%, user's accuracy = 70.14%)

The results of earlier field research suggested that classes "*Calamagrostis villosa* stands" and "*Molinia caeruela* stands" would be confused with each other most often. This assumption was partly confirmed by per-pixel approach; however, also classes "*Nardus stricta* stands" and "*Deschampsia cespitosa* stands" often overlapped. Surprisingly, it was "*Deschampsia cespitosa* stands" that showed the best results of all grassland vegetation – producer's accuracy equalled 70.26%, user's accuracy 40.21% (SVM RBF method).

Regarding the assessment of simplified legend in Western and Eastern Tundra, "*Pinus mugo* scrub" (dense and sparse) again showed the bests results. The producer's accuracy exceeded 90% in both cases; user's accuracy ranged around 60%. However, "*Pinus mugo* scrub dense" was often confused with "*Pinus mugo* scrub sparse". For future WV-2 classification, it may be appropriate to merge these two classes.

In the Western Tundra, "block fields and anthropogenic areas" and "closed alpine grasslands dominated by *Nardus stricta*" showed very good results. Classes "Alpine heathlands" and "block fields and anthropogenic areas" performed best in the East.

4.3 Classification results: per-pixel approach applied to Landsat data

Landsat data were classified only by per-pixel algorithms that were applied to simplified legend, simultaneously in both parts of the tundra. MLC algorithm brought the best results (overall accuracy 78.31%); other algorithms brought worse results by more than 10%.

The classes "*Pinus mugo* srub dense", "Alpine heathlands", "*Picea abies* stands", and "block fields and anthropogenic areas" were classified without major problems – producer's and user' accuracy exceeded 80% and often were close to 100%. In the case of "*Pinus mugo* scrub sparse", producer's accuracy equals 100%, but user's accuracy was rather low (45.9%). It means that "*Pinus mugo* scrub sparse" was overclassified, largely to the detriment of "grasses (except *Nardus stricta*) and subalpine *Vaccinium* vegetation". On the contrary, the class "closed alpine grasslands dominated by *Nardus stricta*" showed a sort of a reverse effect: the producer's accuracy was rather low (44.44%) as the latter was often confused with "grasses (except *Nardus stricta*) and subalpine *Vaccinium* vegetation".

It can be concluded that most problems were posed by grassland vegetation and by classes where grassland vegetation occurs extensively. Other land cover types were classified well also by Landsat data.

4.4 Classification results: map outputs

Classification map outputs can be found in Colour Appendix. Figure 4 shows the best classification results for detailed legend; Figures 5 and 6 show that for simplified legend and object based classification of orthoimages and WordView-2 data in Western and Eastern Tundra. The best results for Landsat 8 data are shown in Figure 7.

When classification outputs are compared, varying spatial resolution of different data types is instantly recognizable. Based on different spatial resolution final mosaics of classified categories differs (areal extent, spatial distribution, shape). While Landsat 8 data are useful rather for general overview, orthoimages provide accurate maps of land cover within the study area for all classes of the detailed legend.

5. Discussion and Conclusions

The major aim of this study was to assess and compare the potential of selected multispectral data with various spatial and spectral resolutions for land cover classification above the tree line. Different types of classifiers were used including per-pixel and object based approach.

Though vegetation types are usually well defined and do not overlap too much in the tundra of Krkonoše, a vast array of species exists there. These species often alternate with each other within a limited area. Consequently, spatial resolution plays a more important role than spectral resolution in the case of object based classification. It was the object based classification of orthoimages (spatial resolution 12.5 cm, four spectral bands) that brought the best results for both legends – overall accuracy equalled 72–84%. Thus, it has been confirmed that application of object based classification is more appropriate than per-pixel approach when data with very high spatial resolution are examined. Orthoimages and object based classification can be recommended to National Park authorities as appropriate tools for landscape monitoring in this area of high nature value. Another advantage is that orthoimages are updated every second year by the state and consequently available for free to the National Park management. On the contrary, object based classification requires a specialized software, the classification itself is rather difficult, and processing time quite long.

The object based classification of WorldView-2 data was less accurate than in the case of orthoimages (68.4% at best) though WV-2 data provide better spectral resolution. The per-pixel approach applied to WV-2 data (detailed legend) was even less accurate; the highest accuracy (60.82%) brought the SVM (RBF) algorithm.

Classification of Landsat data applied to simplified legend (MLC method) brought surprisingly good results – overall accuracy equalled 78%. Construction of the legends may be the reason why per-pixel classifications applied to simplified legend were more accurate in the case of Landsat data rather than for WV-2 data. A special simplified legend optimized for Landsat data was created. The use of training or validation polygons for detailed legend proved to be impossible as in most cases these polygons were smaller than the pixel size (30 × 30 metres); thus, clear pixels for detailed legend could not be defined.

Such a simplified, specially adjusted legend, however, was not fully appropriate for WorldView-2 data. Classes "*Pinus mugo* scrub dense" and "*Pinus mugo* scrub sparse" posed biggest problems in the case of simplified legend and were often confused with each other. Though such a precise definition of *Pinus mugo* (dense vs. sparse) is essential for Landsat data, it is apparently not appropriate for high resolution data as WV-2. Moreover, some training and validation polygons were covered by clouds during research time; consequently, part of WV-2 data could not be used.

This study also compared the suitability of per-pixel and object based classification for different data types. Per-pixel classification proved to be fully appropriate in the case of Landsat data. On the contrary, per-pixel classification of high resolution orthoimages brought unsatisfactory results. Object based classification of Landsat data (spatial resolution 30 metres) does not make much sense either on such a small territory where vegetation classes alternate often. Both types of classification were applied to WorldView-2 data; object based classification brought better results by some 10% than the per-pixel one.

Different algorithms for per-pixel classification were compared, too. The examination of WV-2 data showed that the MLC classifier worked best for simplified legend. In the case of detailed legend, however, the more sophisticated algorithm, SVM (RBF), brought better results.

Earlier field research suggested that classifications would be more accurate in the Eastern Tundra as different vegetation types as specified in the legends seemed to be clearly defined there. As an example, "*Molinia caeruela* stands" and "*Calamagrostis villosa* stands" covered compact areas surrounded by "*Nardus stricta* stands". This presumption was confirmed by orthoimages classification (overall accuracy 83.56%). Classification of WV-2 data, however, brought different results – in part probably due to clouds and shadows on the image.

Classification results may be influenced by varying weather conditions, and also by the season. Vegetation classes tend to be rather compact during spring and autumn, while in summer (July, August) the grassland vegetation advances and different types blend. The blossom may also influence spectral bands in some cases. The above mentioned differences may have played a certain role when orthoimages and WV-2 data were compared. Unfortunately, it is practically impossible to acquire all required multispectral data of different spectral and spatial resolution within one year and one season. That is why it was necessary to examine data acquired in different years. Research results may be partly influenced by this fact.

Regarding classification accuracy of different classes, all types of data brought good results for non-vegetation classes (block fields and anthropogenic areas, water areas). Also the category subalpine *Vaccinium* vegetation shows high accuracy for detailed legend (orthoimages and WV-2 data). As expected, subalpine tall grasslands subcategories with similar spectral signatures (*Calamagrostis villosa* stands and *Deschampsia cespitosa* stands, *Molinia caeruela* stands) show less satisfactory results. The worse-than-expected results in the case of alpine heathlands were probably influenced by the low presence of training polygons. On the contrary, Landsat 8 data covered the whole tundra and therefore also more training polygons – consequently, alpine heathlands were classified with high accuracy (MLC: user's accuracy 95.65%, producer's accuracy 81.48%).

Pinus mugo scrub usually shows good classification results, too. In the case of simplified legend, *Pinus mugo* scrub was further subdivided into dense and spare subcategories; such a subdivision, however, proved to be inappropriate for WV-2 data and orthoimages. As Landsat data consist of rather big pixels, it is difficult to find really uniform categories. *Pinus mugo* scrub sparse is often mixed with grassland vegetation within one pixel. *Pinus mugo* scrub dense does not have this problem and brings better results when classified as a separate class. When it comes to very high resolution data, however, *Pinus mugo* scrub practically does not mix with other categories. Some categories of simplified legend may be too broadly defined for high resolution data. This was proved to a certain extent in the case of closed alpine grasslands dominated by *Nardus stricta* and grasses (except *Nardus stricta*) and subalpine *Vaccinium* vegetation classes.

The results comparing detailed and simplified legends show that in the case of multispectral data with different spatial resolution it is difficult – if not impossible – to find such a compromise that would be appropriate for data of different resolution. One single legend cannot serve a basis for comparison of different data; the level of detail should always be related to data resolution.

It can be concluded that in the case of simplified legend – the overall accuracy of Landsat data (MLC algorithm, 78.31%) and object based classification of orthoimages (83.56%) – our results are similar to those mentioned in earlier scientific sources. As an example, Müllerová (2004) classified multispectral data in Krkonoše in 1986, 1989, and 1997; supervised classification identified nine classes of local vegetation with accuracy 81.1%. Král (2009) classified alpine vegetation on the Czech territory, too. In the latter case, the accuracy of orthoimages equalled 78% (MLC method). However, the rather high spectral variation of different land cover classes and low spectral resolution of orthoimages resulted in mixed character of many classes. Wundram a Loffler (2008) classified alpine vegetation in Norway and achieved similar results. The maximum likelihood method applied to orthoimages (RGB bands) resulted in overall accuracy equalling 51%.

Algorithm MLC used for Landsat data classification brought the accuracy of 78.31% in our research. Knorn et al. (2009) utilized Landsat data for land cover classification in the Carpathians; SVM method brought accuracy up to 98.9% for nine classes. Landsat data were also used by Johansen et al. (2012) for tundra mapping on Svalbard. The final product was a map (scale 1: 500,000) containing eighteen classes. The processing chain contained six stages including unsupervised classification and merging the classes based on ancillary data. Verification of the final product is problematic in such remote areas; the overlap between Landsat data classification and traditional vegetation mapping in Gipsdalen Valley reached 55.36% (eight aggregated classes were tested).

Our research confirms that Landsat data are sufficient to get a general overview of basic land cover classes above the tree line in the Krkonoše Mts. National Park. Alternatively, the recently launched Sentinel-2 satellite could be used – images have comparable spatial resolution and better spectral resolution. Detailed classification, however, requires orthoimages with very high spatial resolution, plus sophisticated algorithms of object based classification should be used. WorldView-2 data brought the least satisfactory results in our research. However, this may have been influenced by clouds, and also by problems with exact definition of the legend as discussed above. Based on the comparison of the data with different spectral and spatial resolution we can conclude that very high spatial

resolution is the decisive feature that is essential to reach high overall classification accuracy in the detailed level. Zagajewski (2005) and other scientists suggest that utilization of hyperspectral data of very high spatial resolution (alternatively combined with LiDAR data – see Dalponte 2012) could bring further improvements of classification accuracy.

Acknowledgements

This research was made possible by the support of The Charles University in Prague Grant Agency: GAUK project No. 938214 – Remote sensing for classification of vegetation above tree-line in the Krkonoše Mts.National Park. Our grateful thanks go also to RNDr. Stanislav Březina, PhD., and Mgr. Jan Šturma who helped to carry out botanical research and to create the legends.

REFERENCES

BENEDIKTSSON, J. A., SWAIN, P. H., ERSOY, O. K. (1990): Neural network approaches versus statistical methods in classification of multisource remote sensing data. IEEE Transactions on geoscience and remote sensing 28(4), 540–551. http://dx.doi.org/10.1109/TGRS.1990.572944

BLASCHKE, T. (2010): Object based image analysis for remote sensing. ISPRS Journal of Photogrammetry and Remote Sensing 65(1), 2–16. http://dx.doi.org/10.1016/j.isprsjprs.2009.06.004

CAMPS-VALLS, G., GÓMEZ-CHOVA, L., CALPE-MARAVILLA, J. (2004): Robust support vector method for hyperspectral data classification and knowledge discovery. IEEE Transactions on geoscience and remote sensing, Valencia, 20, pp. 1–13. http://dx.doi.org/10.1109/tgrs.2004.827262

CLEVE, C., KELLY, M., FAITH, R. K., MORITZ, M. (2008): Classification of the wildland–urban interface: A comparison of pixel and object-based classifications using high-resolution aerial photography. Computers, Environment and Urban Systems 32, 317–326. http://dx.doi.org/10.1016/j.compenvurbsys.2007.10.001

DALPONTE, M., BRUZZONE, L., GIANELLE, D. (2012): Tree species classification in the Southern Alps based on the fusion of very high geometrical resolution multispectral/hyperspectral images and LiDAR data. Remote sensing of Environment 123, 258–270. http://dx.doi.org/10.1016/j.rse.2012.03.013

DIXON, B., CANDADE, N. (2008): Multispectral landuse classification using neural networks and support vector machines: one or the other, or both? International Journal of Remote Sensing 29(4), 1185–1206. http://dx.doi.org/10.1080/01431160701294661

DUARTE, C. M., MIDDELBURG, J. W., CARACO, N. (2005): Major role of marine vegetation on the oceanic carbon cycle. Biogeosciences 2(1), 1726–4170. http://dx.doi.org/10.5194/bg-2-1-2005

FERNANDEZ-PRIETO, D., ARINO, O., BORGES, T., DAVIDSON, N., FINLAYSON, MAX, GRASSL, H., MACKAY, H., PRIGENT, C., PRITCHARD, D., ZALIDIS, G. (2006): The globwetland symposium: summary and way forward. Proc. Glob-Wetland: Looking at Wetlands from Space. ESA Publications Division, Frascati, pp. 19–20.

CHYTRÝ, M., KUČERA, T., KOČÍ, M., GRULICH, V., LUSTYK, P. (2001): Katalog biotopů České republiky. Praha: AOPK ČR.

JENÍK, J., ŠTURSA, J. (2003): Vegetation of the Giant Mountains, Central Europe. In: NAGY, L., GRABHERR, G., KÖRNER, CH., THOMPSON, D. B. A. (eds.), Alpine Biodiversity in Europe (Ecology Studies Vol. 167), New York: Springer, pp. 47–51.

JOHANSEN, B. E., KARLSEN, S. R., TØMMERVIK, H. (2012): Vegetation mapping of Svalbard utilising Landsat TM/ETM+ data. Polar Record 48, 47–63. http://dx.doi.org/10.1017/s0032247411000647

JONES, H. G., VAUGHAN, R. A. (2010): Remote sensing of vegetation: Principles, techniques and applications. Oxford: Oxford University Press.

KNORN, J., RABE, A., RADELOFF, V. C., KUEMMERLE, T., KOZAK, J., HOSTERT, P. (2009): Land cover mapping of large areas using chain classification of neighboring Landsat satellite images. Remote Sensing of Environment 113(5), 957–964. http://dx.doi.org/10.1016/j.rse.2009.01.010

KRÁL, K. (2009): Classification of current vegetation cover and alpine treeline ecotone in the Praděd Reserve (Czech Republic), using remote sensing. Mountain Research and Development 29(2), 177–183. http://dx.doi.org/10.1659/mrd.1077

LALIBERTE, A. S., RANGO, A., HERRICK, J. E., FREDRICKSON, E. L., BURKETT, L. (2007): An object-based image analysis approach for determining fractional cover of senescent and green vegetation with digital plot photography. Journal of Arid Environments 69(1), 1–14. http://dx.doi.org/10.1016/j.jaridenv.2006.08.016

LANTZ, T. C., GERGEL, S. E., KOKELJ, S. V . (2010): Spatial Heterogeneity in the Shrub Tundra Ecotone in the Mackenzie Delta Region, Northwest Territories. Implications for Arctic Environmental Change. Ecosystems, 13/2, pp. 194-204, http://dx.doi.org/10.1007/s10021-009-9310-0

LOKVENC, T. (1995): Analysis of anthropogenic changes of woody plant stands above the alpine timber line in the Krkonoše Mts. Opera Corcontica 32, 99–114.

MARCINKOWSKA, A., ZAGAJEWSKI, B., OCHYTRA, A., JAROCIŃSKA, A., RACZKO, E., KUPKOVÁ L., ŠTYCH, P., MEULEMAN, K. (2014): Mapping vegetation communities of the Karkonosze National Park using APEX hyperspectral data and Support Vector Machines. Miscellanea Geographica 18(2), 23–29. http://dx.doi.org/10.2478/mgrsd-2014-0007

MARGOLD, M., TREML, V., PETR, L., NYPOLOVÁ, P. (2011): Snowpatch hollows and pronival ramparts in the Krkonoše Mountains, Czech Republic: distribution, morphology and chronology of formation. Geografiska Annaler, Ser. A Physical Geography 93, 137–150. http://dx.doi.org/10.1111/j.1468-0459.2011.00422.x

MOUNTRAKIS, G., IM, J., OGOLE, C. (2011): Support vector machines in remote sensing: A review; ISPRS Journal of Photogrammetry and Remote Sensing 66, 247–259. http://dx.doi.org/10.1016/j.isprsjprs.2010.11.001

MÜLLEROVÁ, J. (2005): Use of digital aerial photography for subalpine vegetation mapping: A case study from the Krkonoše Mts., Czech Republic. Plant Ecology 175(2), 259–272. http://dx.doi.org/10.1007/s11258-005-0063-3

MYINT, S. W., GOBER, P., BRAZEL, A., GROSSMAN-CLARKE, S., WENG, Q. (2011): Per-pixel vs. object-based classification of urban land cover extraction using highspatial resolution imagery. Remote Sensing of Environment 115, 1145–1161. http://dx.doi.org/10.1016/j.rse.2010.12.017

NOVÁK, J., PETR, L., TREML, V. (2010): Late-Holocene human-induced changes to the extent of alpine areas in the East

Sudetes, Central Europe. The Holocene 20, 895–905. http://dx.doi.org/10.1177/0959683610365938
PATTISON, R. R., JORGENSON, J. C., RAYNOLDS, M. K., WELKER, J. M. (2015): Trends in NDVI and tundra community composition in the Arctic of NE Alaska between 1988 and 2009. Ecosystems 18, 707–719. http://dx.doi.org/10.1007/s10021-015-9858-9
PETROPOULOS, G. P., ARVANITIS, K., SIGRIMIS, N. (2012): Hyperion hyperspectral imagery analysis combined with machine learning classifiers for land use/cover mapping. Expert Systems with Applications 39, 3800–3809. http://dx.doi.org/10.1016/j.eswa.2011.09.083
RESLER, L. M., FONSTADA, M. A., BUTLERA, D. R. (2004): Mapping the alpine treeline ecotone with digital aerial photography and textural analysis. Geocarto International 19(1), 37–44. http://dx.doi.org/10.1080/10106040408542297
SONG, C., WOODCOCK, C. E., SETO, K. C., PAX LENNEY, M., MACOMBER, S. A. (2001): Classification and change detection using Landsat TM data: When and how to correct atmospheric effects? Remote Sensing of Environment 75(2), 230–244. http://dx.doi.org/10.1016/S0034-4257(00)00169-3
SOUKUPOVÁ, L., KOCIÁNOVÁ M., JENÍK, J., SEKYRA, J. (1995): Arctic alpine tundra in the Krkonoše, the Sudetes. Opera Corcontica 32, 5–88.
SPERANZA, A., HANKE, J., VAN GEEL, B., FANTA, J. (2000): Late-Holocene human impact and peat development in the Černá hora bog, Krkonoše Mountains, Czech Republic. Holocene 10, 575–585. http://dx.doi.org/10.1191/095968300668946885
TREML, V., JANKOVSKÁ, V., PETR, L. (2008): Holocene dynamics of the alpine timberline in the High Sudetes. Biologia 63, 73–80. http://dx.doi.org/10.2478/s11756-008-0021-3
WOLTER, P. T., MLADENOFF D. J., HOST, G. E., CROW, T. R. (1995): Improved Forest classification in the Northern Lake states using multitemporal Landsat imagery. Photogrammetric Engineering and Remote Sensing 61(9), 1129–1143.
WUNDRAM, D., LOFFLER, J. (2008): High-resolution spatial analysis of mountain landscapes using a lowaltitude remote sensing approach. International Journal of Remote Sensing, University of Bonn, 29.4, pp. 961-974. http://dx.doi.org/10.1080/01431160701352113
YU, Q., GONG, P., CLINTON, N., BIGING, G., KELLY, M., SCHIROKAUER, D. (2006): Object-based Detailed Vegetation Classification with Airborne High Spatial Resolution Remote Sensing Imagery. Photogrammetric Engineering and Remote Sensing 72(7), 799–811. http://dx.doi.org/10.14358/PERS.72.7.799
ZAGAJEWSKI, B., KOZLOWSKA, A., KROWCZYNSKA, M., SOBCZAK, M., WRZESIEN, M. (2005): Mapping high mountain vegetation using hyperspectral data. EARSeL eProceedings 4(1), 70–78.

RESUMÉ

Klasifikace vegetace nad horní hranicí lesa v Krkonošském národním parku s využitím multispektrálních dat

Článek hodnotí možnosti multispektrálních dat s rozdílným prostorovým a spektrálním rozlišením pro klasifikaci vegetace nad horní hranicí lesa v Krkonošském národním parku. Letecká ortofota s velmi vysokým prostorovým rozlišením 12,5 cm a čtyřmi spektrálními pásmy byla klasifikována objektovou klasifikací. Družicová data WorldView-2 (WV-2) s vysokým prostorovým rozlišením 2 m a osmi spektrálními pásmy byla klasifikována jak objektově, tak pixelově. Pixelová klasifikace byla provedena i na volně dostupných datech Landsat 8 s prostorovým rozlišením 30 m a sedmi spektrálními pásmy. Z algoritmů pro pixelovou klasifikaci byly porovnávány klasifikátory maximum likelihood classification (MLC), support vector machine (SVM) a neural net (NN). Pro objektovou klasifikaci byl využíván přístup example-based a algoritmus SVM (vše dostupné v ENVI 5.2). Schéma pracovního postupu je na obrázku 3.

Analýza byla provedena v krkonošské tundře. Modelová oblast je situována ve dvou prostorově oddělených částech – východní a západní části tundry (obrázek 1). Pomocí dat Landsat byla hodnocena celá oblast východní (rozloha 1284 ha) i západní (rozloha 2284 ha) tundry v české části KRNAP. Pomocí ostatních datových zdrojů vzhledem k výpočetní náročnosti klasifikací pouze vybrané části území (565 ha na západě v and 839 ha na východě) reprezentativní pro danou oblast.

Klíčovou částí práce byla definice legendy, která byla vytvořena ve spolupráci s botanikem Krkonošského národního parku. Základní podrobná legenda obsahuje celkem 12 tříd (viz níže a viz obrázek 2). Byla využita pro ortofota a WV-2, a to pouze v západní tundře. Vzhledem k tomu, že se dané třídy vyskytují velmi často na menších plochách, než je pixel Landsatu 8 (tj. 900 m^2), bylo nutné vytvořit i zjednodušenou legendu vhodnou pro klasifikaci dat Landsat. Zjednodušená legenda obsahuje 8 tříd a byla použita pro klasifikaci všech zmíněných typů dat za účelem jejich porovnání.

Podrobná legenda
1. kamenná moře a antropogenní plochy
2. smrkové porosty
3. kosodřevina
4. subalpínská brusnicová vegetace
5. alpínské trávníky zapojené
5a. smilka tuhá
5b. druhově bohaté porosty s vysokým zastoupením dvouděložných
6. subalpínské vysokostébelné trávníky
6a. třtina chloupkatá
6b. bezkolenec modrý
6c. metlice trsnatá
7. subalpínské vysokobylinné trávníky
8. alpínská vřesoviště
9. mokřady a rašeliniště
10. vodní plochy (klasifikovány pouze z ortofot)

Zjednodušená legenda
1. kamenná moře a antropogenní plochy
2. smrkové porosty
3a. kosodřevina hustá (> 80% porostu)
3b. kosodřevina řídká (30% - 80% porostu)
4. alpínské trávníky zapojené s vysokým zastoupením smilky tuhé
5. trávy (vyjma smilky tuhé) a subalpínská brusnicová vegetace
6. alpínská vřesoviště
7. mokřady a rašeliniště
8. vodní plochy (klasifikovány pouze z ortofot)

Nejlepší výsledky byly v případě podrobné i zjednodušené legendy dosaženy pro ortofota (celková přesnost klasifikace 83,56, resp. 71,96 %, Kappa koeficient 0,8, resp. 0,65). Klasifikace WV-2 dosáhla nejlepšího výsledku v případě objektového přístupu a zjednodušené legendy (68,4 %), z pixelových klasifikací v případě metody SVM (RBF) a podrobné legendy (60,82 %). Data Landsat byla nejpřesněji klasifikována s využitím MLC (78,31 %). Nejlepší klasifikační výstupy pro jednotlivé typy dat jsou na obrázcích 4–7.

Potvrdil se náš předpoklad, že v případě vegetace v tundře dosáhneme pro data s velmi vysokým prostorovým rozlišením objektovou klasifikací lepších výsledků než klasifikací pixelovou. Ortofota a objektovou klasifikaci lze na základě našich výsledků doporučit managementu národního parku pro monitoring této cenné části Krkonoš. Výhodou je i to, že ortofota jsou pravidelně každé dva roky pořizována ze státních zdrojů a národní parky je mají volně k dispozici. Nevýhodou je naopak nutnost vlastnit SW pro objektovou klasifikaci, poměrně náročný postup klasifikace a delší výpočetní čas.

Pokud se týká přesnosti klasifikace jednotlivých tříd, tak lze říci, že v žádném z typů dat nebyl problém s klasifikací nevegetačních tříd (kamenná moře a antropogenní plochy, vodní plochy). Dobře byla také většinou vyklasifikována kategorie kosodřevina. Pro detailní legendu dosahovala dobré přesnosti také kategorie subalpínská brusnicová vegetace (v případě ortofot i WV-2). Horší klasifikační výsledky jsme podle očekávání zaznamenali v případě podkategorií třídy subalpínské vysokostébelné trávníky, jejichž spektrální signál je podobný (třtina chloupkatá, bezkolenec modrý, metlice trsnatá).

Na základě výsledků klasifikace jednotlivých kategorií s využitím podrobné a zjednodušené legendy lze učinit závěr, že v případě klasifikace multispektrálních dat s řádově různým prostorovým rozlišením je problém najít takovou kompromisní legendu, která by vyhovovala všem prostorovým rozlišením. Srovnání potenciálu těchto dat na základě jedné legendy tedy není zcela možné a při sestavování legendy vždy musíme její podrobnost vztáhnout k rozlišení dat.

Z porovnání dat s rozdílným spektrálním a prostorovým rozlišením vyplynulo, že velmi vysoké prostorové rozlišení dat je zásadním parametrem pro dosažení vysoké celkové přesnosti klasifikace v detailní úrovni.

Renáta Suchá, Lucie Jakešová, Lucie Kupková,
Lucie Červená
Charles University in Prague, Faculty of Science
Department of Applied Geoinformatics and Cartography
Albertov 6, 128 43 Praha 2
Czech Republic
E-mail: renata.sucha@natur.cuni.cz,
jakesova-lucie@seznam.cz
lucie.kupkova@gmail.com
lucie.cervena@natur.cuni.cz

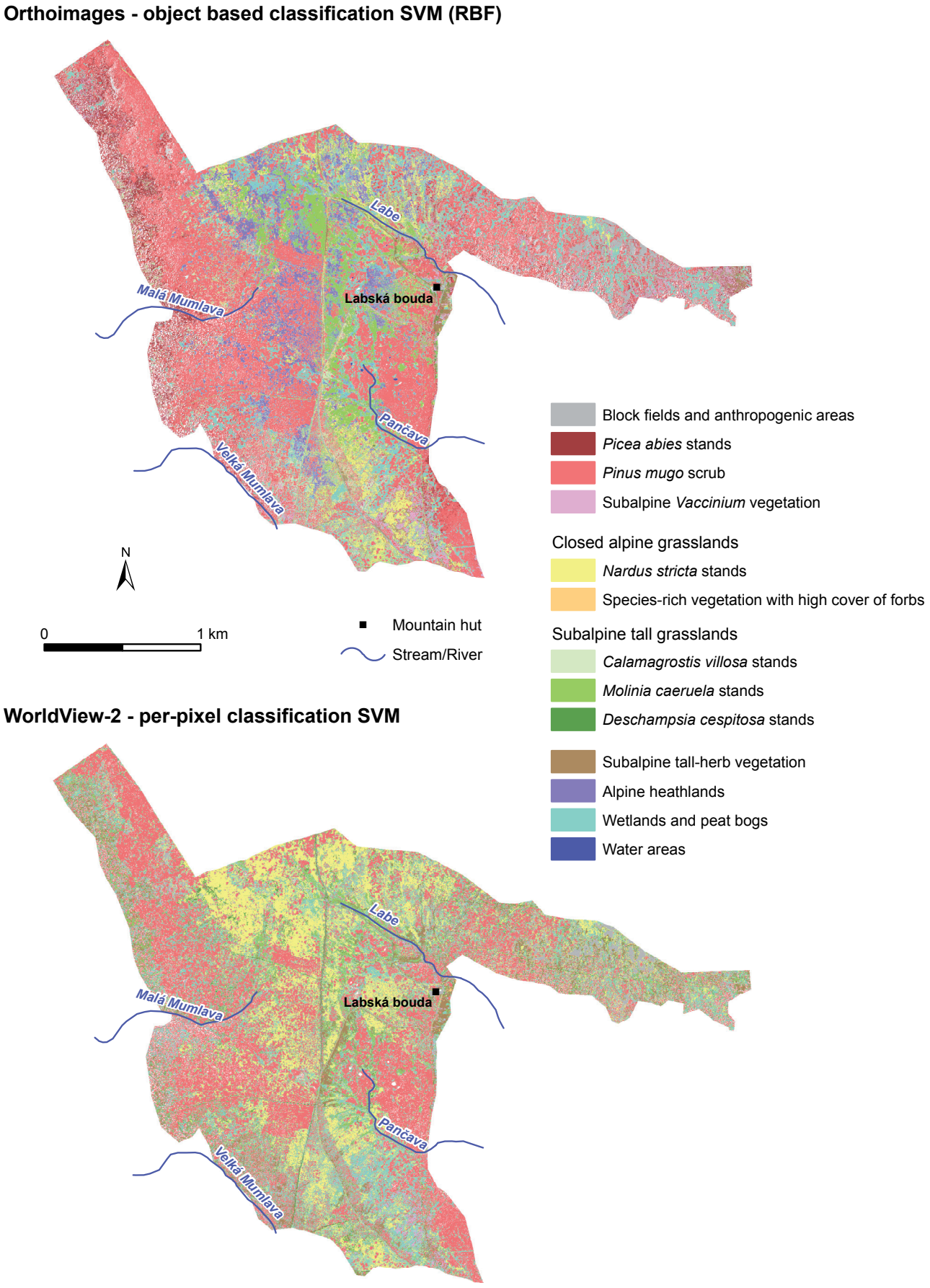

Fig. 4 Classification results for **detailed legend** in **Western** Tundra. Upper figure: **orthoimages – object based** classification SVM (RBF); lower figure: **WordView-2** – **per-pixel** classification SVM (RBF). Source: Authors

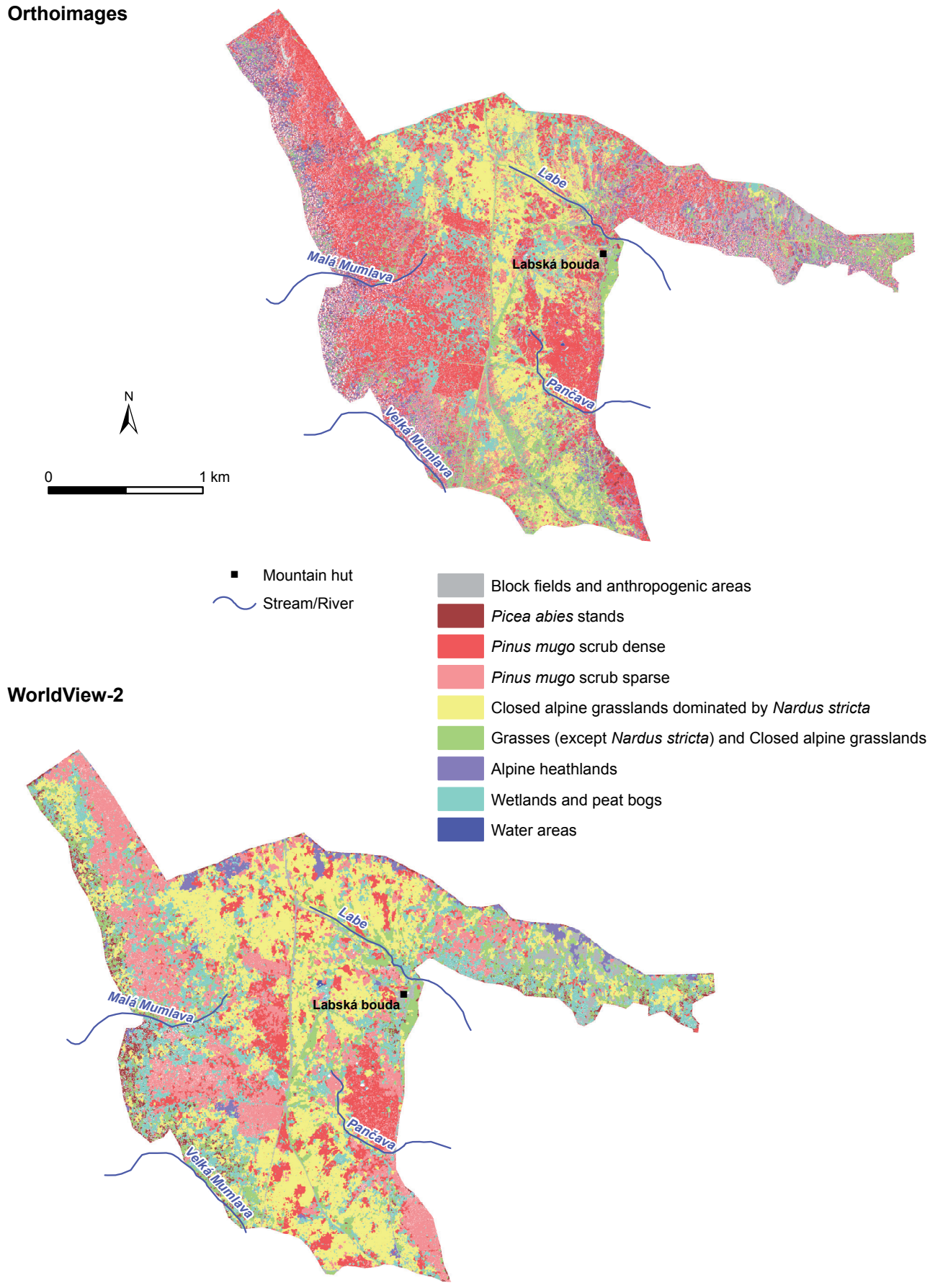

Fig. 5 Results of object based classification SVM (RBF) for **simplified legend** in **Western** Tundra. Upper figure **orthoimages**, lower figure **WordView-2**. Source: Authors

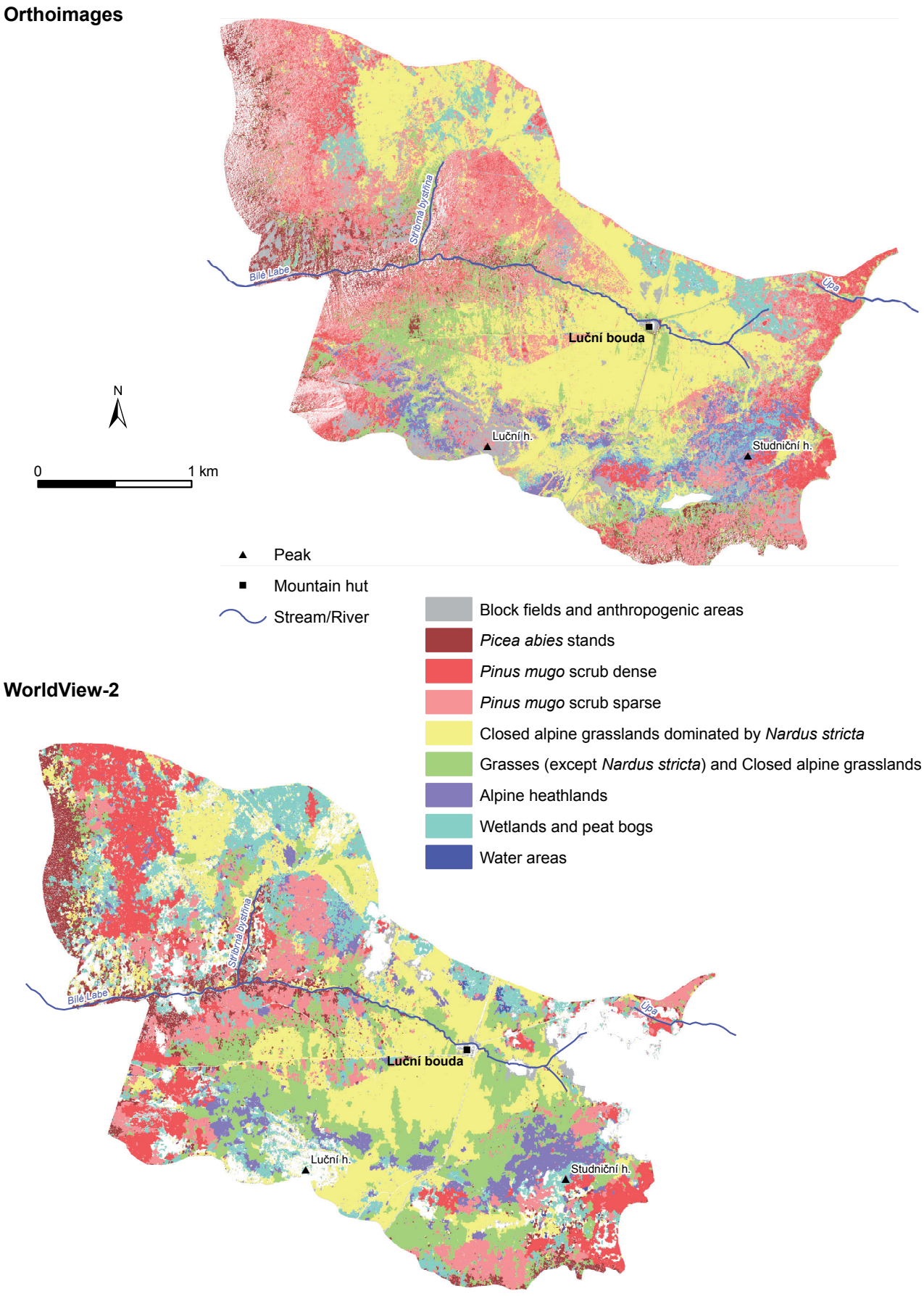

Fig. 6 Results of object based classification SVM (RBF) for **simplified legend** in **Eastern** Tundra. Upper figure **orthoimages**, lower figure **WordView-2**. Source: Authors

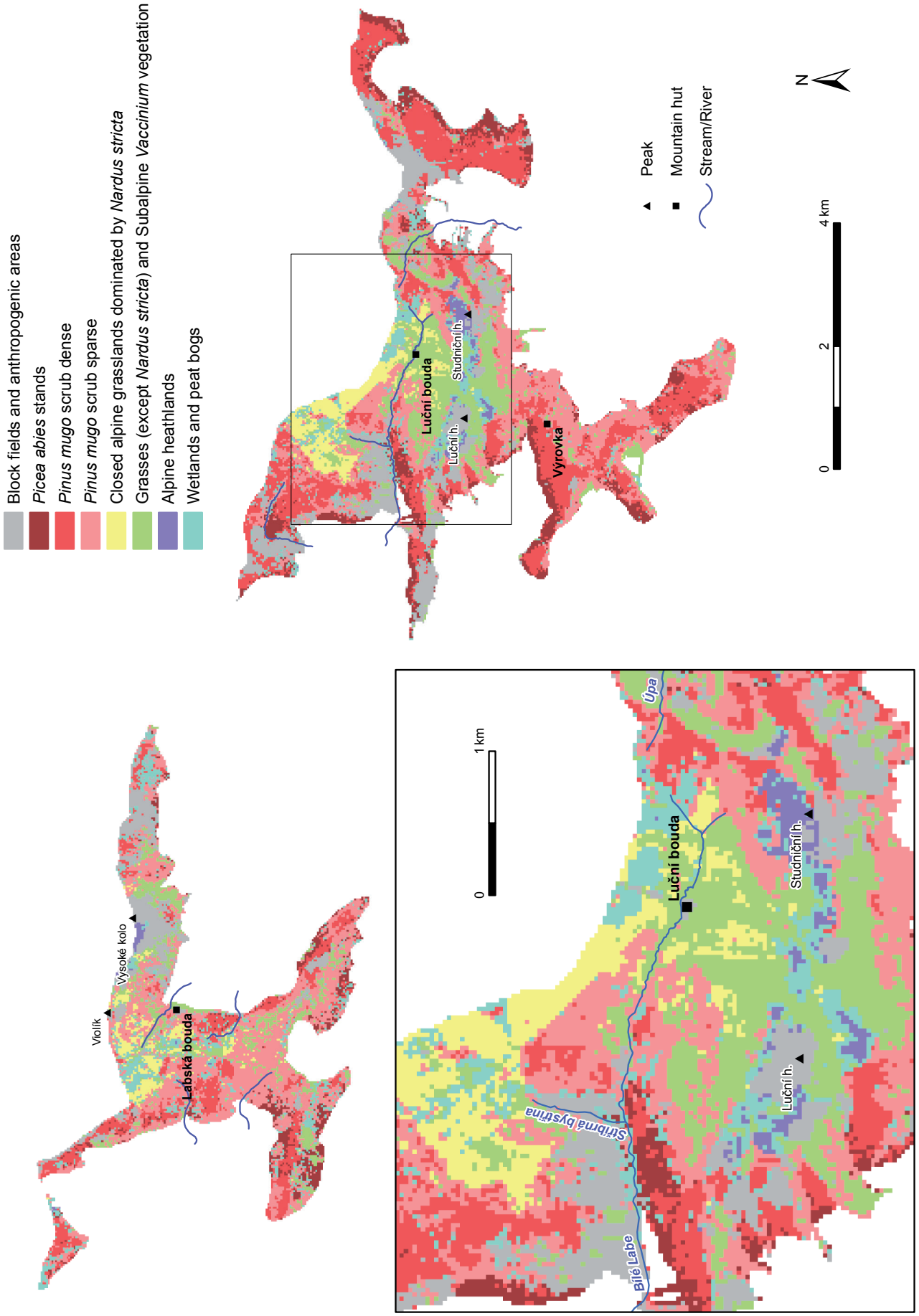

Fig. 7 Classification results for **Landsat 8** – maximum likelihood classifier. Source: Authors